A Study on the Effects of SEBS-*g*-MAH on the Phase Morphology and Mechanical Properties of Polypropylene/ Polycarbonate/SEBS Ternary Polymer Blends

O. Moini Jazani,[1] A. Arefazar,[1] S. H. Jafari,[2] M. H. Beheshty,[3] A. Ghaemi[1]

[1]*Polymer Engineering Department, Amir Kabir University of Technology, Tehran, Iran*
[2]*School of Chemical Engineering, University of Tehran, Tehran, Iran*
[3]*Composites Department, Iran Polymer and Petrochemical Institute, Tehran, Iran*

Received 3 December 2010; accepted 27 September 2010
DOI 10.1002/app.33715
Published online 29 March 2011 in Wiley Online Library (wileyonlinelibrary.com).

ABSTRACT: In this work, five ternary blends based on 70% by weight (wt %) of polypropylene (PP) with 30% wt of polycarbonate (PC)/poly(styrene-*b*-(ethylene-*co*-butylene)-*b*-styrene)(SEBS) dispersed phase consists of 15 wt % PC and 15 wt % reactive (maleic anhydride grafted) and nonreactive SEBS mixtures at various ratios were prepared in a co-rotating twin screw extruder. scanning electron microscopy (SEM) micrographs showed that the blends containing only nonreactive SEBS exhibited a fine dispersion of core-shell particles. With decreasing the SEBS/SEBS-*g*-Maleic Anhydride (MAH) weight ratio, the morphology changed from the core-shell particles to a mixed of core-shell, rod-like and individual particles. This variation in phase morphology affected the thermal and mechanical properties of the blends. DSC results showed that the blends containing only nonreactive SEBS exhibited a minimum in degree of crystallinity due to the homogeneous nucleation of core-shell particles. Mechanical testing showed that in the SEBS/SEBS-*g*-MAH weight ratio of 50/50, the modulus and impact strength increased compared with the PP matrix while the yield stress had minimum difference with that of PP matrix. These effects could be attributed to the formation of those especial microstructures revealed by the SEM studies. © 2011 Wiley Periodicals, Inc. J Appl Polym Sci 121: 2680–2687, 2011

Key words: ternary blends; morphology; mechanical properties; reactive compatibilization

INTRODUCTION

In the past decades, there have been active research interests in the study of polymer blends. Because most polymers are thermodynamically immiscible, blending polymers without compatibilizers do not lead to enhanced properties of the final products. It is widely known that the presence of compatibilizers could moderate, to some extent, these problems by affecting the interfacial activities.[1,2] Compatibilization of polymer blends has been extensively used in recent studies using graft or block copolymers with segments potential of establishing intermolecular attractions and/or chemical reactions with blend constituents.[3] In both polypropylene (PP)/polyamide-6 (PA-6) binary and PP/PA-6/Poly(styrene-*b*-(ethylene-*co*-butylenes)-*b*-styrene) (SEBS) ternary blend systems, using maleated SEBS (SEBS-*g*-Maleic Anhydride (MAH) as the compatibilizer, strongly influenced the blend morphology and mechanical properties by affecting the degree of interfacial reaction between the succinic anhydride groups of the SEBS-*g*-MAH and the terminal amino groups of PA6.[3–6] Nikos et al. demonstrated that the morphology and mechanical properties of high density polyethylene/poly(ethylene-*co*-vinyl alcohol) binary blends is strongly influenced by SEBS-*g*-MAH as the compatibilizer.[7] In polypropylene (PP)/polycarbonate (PC) binary systems, polypropylene grafted with glycidyl methacrylate(PP-*g*-GMA) significantly affected the morphological, thermal, rheological, and mechanical properties[8] Huang et al. studied ternary polymer blends based on polyamide6 (PA6)/ethylene propylene rubber (EPR)/maleated ethylene propylene rubber (EPR-*g*-MAH) and suggested that the blend morphology strongly depends on the degree of maleation in the rubber phase[9] Wang et al. evaluated thermal and morphological properties of polyamid12/poly(butylene terephthalate)(PBT)blends with hyperbranched poly (ethylene imine)-*g*-polyamid12(PET-*g*-PA12) as reactive compatibilizer. They showed that the addition of poly(ethylene imine) (PEI)-*g*-PA12 strongly affected the morphology of PA12/PBT blends, which were originally an incompatible polymer pair.[10] Yin et al. studied the effects of styrene-*b*-(ethylene-*co*-butylene)-*b*-styrene (SEBS) triblock copolymer functionalized with ε-caprolactam blocked allyl(3-isocyanate-4-tolyl)

Correspondence to: A. Arefazar (arefazar@aut.ac.ir).

© 2011 Wiley Periodicals, Inc.

carbamate(SEBS-*g*-BTAI) on the morphology and mechanical properties of PA6/SEBS blends. Smaller dispersed particle sizes with narrow distribution were found in PA6/SEBS blends. Also, mechanical properties such as tensile strength, Young modulus, and Izod impact strength of PA6/SEBS-*g*-BTAI were improved distinctly with respect to PA6/SEBS blends.[11] Wang et al. showed that in ternary polymer blends based on polypropylene (PP)/nylon11/maleated ethylene propylene-diene rubber (EPDM-*g*-MAH), the dispersed phase morphology of maleated elastomer was hardly affected by addition of nylon11, whereas dispersed phase domains of nylon11 strongly influenced by the maleated elastomer loading. The results of mechanical properties showed that the ternary blends exhibited inferior tensile strength in comparison with the PP matrix, but superior toughness.[12] Kusmono et al. demostrated that the incorporation of SEBS-*g*-MAH in to the nanocomposites based on polyamide6 (PA6)/polypropylene(PP) blends containing organophilic montmorillinite increased strength, ductility, and impact strength but slightly decreased stiffness.[13] Denac et al. studied the structure-mechanical properties relationships upon the SEBS and SEBS-*g*-MAH content in the isotactic polypropylene(iPP)/talc/styrenic rubber block copolymer composites. It has been observed SEBS-*g*-MAH encapsulated and disoriented plane-parallel talc crystals more significantly than the SEBS. Mechanical properties and their relation with the morphology of composites explained by observed differences between the SEBS and SEBS-*g*-MAH (molecular weight, elasticity, and viscosity).[14,15] It has been observed that for the blend systems containing two minor phases, three distinct types of phase morphology have to be specified. For some ternary systems, one of the minor components forms an encapsulating layer around domains of another minor component, whereas in other systems two minor components form independent phases separately. The third type is the intermediate case, where mixed phases of the two components are formed without any ordered structures.[16–22] To predict the tendency of one minor phase to encapsulate the second one, the alternate form of Harkin's equation can be used as follows:

$$\lambda_{BC} = \lambda_{AC} - \lambda_{AB} - \lambda_{BC} \quad (1)$$

where γ_{AC}, γ_{AB}, and γ_{BC} are the interfacial tensions for each component pairs, and λ_{BC} is defined as the spreading coefficient for the shell forming component B on the core of component C. The index A corresponds to the matrix continuous phase. If the λ_{BC} is positive the B-phase will encapsulate the C-phase. Similarly,

$$\lambda_{CB} = \lambda_{AB} - \lambda_{AC} - \lambda_{BC} \quad (2)$$

when λ_{CB} is positive, the component C will also encapsulate component B. However, if both λ_{CB} and λ_{BC} are negative, component C and B will tend to form two separate dispersed phases within the matrix component A. In the intermediate region, where $\lambda_{BC} \sim 0$, stack morphology may result, in which component B only partially eliminates the interface between component C and the matrix.[3]

Guo[16] and coworkers presented a new model to predict the morphology of ternary blends. They obtained an equation for the free energy of multicomponent blends, which was dependent on the surface tension and also interfacial area of polymer components. They claimed that the most stable morphology is the one exhibiting the least free energy of all possible pairs. Guo's Relative Interfacial Energy (RIE) equations are as below:

$$(\mathrm{RIE})_{B/C} = \left(\sum A_i\gamma_{ij}\right)_{B/C}/K = (1+x)^{2/3}\gamma_{AB} + \gamma_{BC} \quad (3)$$

$$(\mathrm{RIE})_{C/B} = \left(\sum A_i\gamma_{ij}\right)_{C/B}/K = [x^{2/3}\gamma_{BC} + (1+x)^{2/3}\gamma_{AC}] \quad (4)$$

$$(\mathrm{RIE})_{B+C} = \left(\sum A_i\gamma_{j}\right)_{B+C}/K = x^{2/3}\gamma_{AB} + \gamma_{AC} \quad (5)$$

where x is equal to $x = V_B/V_C$, γ_{ij} is the interfacial tension between two phases and k is a constant. V_B and V_C are volume fractions of B and C phases, respectively. Both models, the spreading coefficient and the minimal free energy surface, have been widely used by different researchers to predict the ternary blends morphology.[3,23–27]

In this study, the effects of SEBS-*g*-MAH on the mechanical and morphological properties are investigated for PP/PC/SEBS ternary polymer blends. According to this aim, a range of blends based on 70% by weight(wt %) of polypropylene(PP) with 30 wt % of PC/SEBS dispersed phase consisting 15 wt % PC and 15 wt % reactive (maleic anhydride grafted) and nonreactive SEBS mixtures at various ratios were prepared using twin co-rotating twin screw extruder. Attention has been focused on the phase morphology and its effect on the mechanical and thermal properties of PP/PC/SEBS ternary blends.

EXPERIMENTAL

Materials

The following materials were used in this research:

An iso-tactic polypropylene homo-polymer (PP), SEETEC H5300 supplied by LG chemical company-(Korea) (MFI: 3.5 g/10 min, 230°C, 2.16 kg), (ii) Polycarbonate (PC), Makrolon® 2858 purchased from Bayer Co.(Germany) (MFI: 10 g/10 min, 300°C, 1.2 kg), (iii) Poly(styrene-*b*-(ethylene-*co*-butylene)-*b*-styrene) (SEBS) tri-block copolymer, Kraton™ G1652 supplied by Shell Chemicals (29% styrene; molecular

TABLE I
Various Compositions of Ternary Polymer Blends

Code No.	PP (wt %)	PC (wt %)	SEBS+ SEBS-*g*-MAH (wt %)	Weight ratio of SEBS to SEBS-*g*-MAH
I1	70	15	15	100/0
I2	70	15	15	75/25
I3	70	15	15	50/50
I4	70	15	15	25/75
I5	70	15	15	0/100

weight; styrene block 7000, EB block 37500, MFI: 5 g/10 min, 5 kg, 230°C); (iv) Maleic-anhydride grafted SEBS (SEBS-*g*-MAH) tri-block copolymer, Kraton^{TM} FG1901x supplied by Shell Chemicals (29% styrene, nominal weight of grafted maleic anhydride = 1.8 ± 0.4%, MFI: 22 g/10 min, 5 kg, 230°C).

Blend preparation

In this study, five ternary blends of PP/PC/ mixed (SEBS+SEBS-*g*-MAH) were produced at different weight ratio of SEBS to SEBS-*g*-MAH using a Brabender co-rotating twin screw extruder (diameter of screw = 2 cm, length/diameter ratio = 40).The various compositions used for this research are reported in Table I. Before processing, the materials were dried in an oven for at least 17 h at 80°C. The barrel of extruder had six temperature-control zones and their temperatures were set at 230–235–240–245–250–255°C (from hopper to die). PP and SEBS-*g*-MAH were first preblended and then extruded with PC and SEBS. The extrudates were quenched in a cooling water bath and pelletized in a granulator. The screw speed was maintained at 130 rpm.

Mechanical properties

The dried pelletized blends were molded to form tensile and impact specimens using an ENGEL injection molding machine. The barrel temperature profile was 180°C (hopper) to 240°C (nozzle) and the mold temperature was maintained at 40°C. Tensile stress-strain data were obtained using a Galdabini testing machine with cross head speed of 50 mm/min according to the ASTM D-638. Moreover Izod impact strength was measured for notched specimens according to ASTM D-256 using a Zwick pendulum-type tester.

Thermal properties

The thermal analysis was carried out using a 200F3Maia differential scanning calorimeter (DSC). Specimens of 5–10 mg in weight were taken from the impact test specimens and subjected to heating-cooling-heating cycles between 30 and 265°C with a heating rate of 10°K/min (kelvin/min) in a nitrogen atmosphere. The percentage of crystallinity(%Xc) was calculated using the following equation:

$$\% \text{ Xc} = \frac{\Delta H_f}{\Delta H_f^0} \times \frac{1}{\omega_{pp}} \times 100 \quad (6)$$

where ΔH_f is the heat of fusion for PP in the corresponding blend and ΔH_f^0 is the heat of fusion of 100% crystalline PP and was taken as 209.2 J/g from the literature.[13,28] ω_{PP} is the weight fraction of PP.

Morphological studies

To evaluate the effect of particle size and the type of resulted morphology on the mechanical properties of PP/PC/SEBS ternary blends, scanning electron microscopy (SEM) micrographs were obtained using an AIS-2100 SEM from supplied by SERON Company through fracture surface of impact specimens. Before the SEM studies, the impact samples were fractured in liquid nitrogen and consequently were etched by cyclohexane for 24 h to remove SEBS and SEBS-*g*-MAH minor phases. Then, the etched samples were gold sputtered to make the samples conductive. Also the ImageJ software was used for image analysis of the SEM micrographs. In ImageJ software, according to the following procedure, we analyzed the images.

First, the software calibrated according to the scale of image (set scale). Second, the required measurement that should be registered in output file of image software is defined, the image opened, and, according to the instruments, started to analyze. Our image consists of individual particles, core shell composite particles and rod-like composite particles. According to zoom of software count visually. After counting, each part is marked to prevent from error and according to defined parameter at calibration stage, output in excel file showed.

RESULTS AND DISCUSSION

Interfacial tension

The interfacial tension coefficients were obtained using harmonic mean equation as:

$$\gamma_{12} = \gamma_1 + \gamma_2 - \frac{4\gamma_{1d}\gamma_{2d}}{\gamma_{1d} + \gamma_{2d}} - \frac{4\gamma_{1p}\gamma_{2p}}{\gamma_{1p} + \gamma_{2p}} \quad (7)$$

where γ, γ_d and γ_p are surface tension, dispersive contribution of γ and polar contribution of γ at 255°C. Table II presents γ, γ_d and γ_p for PP, PC, and SEBS at 255°C calculated on the basis of data reported in Refs. 3,30–32. As EB is the major part of SEBS chains, the surface tension of this component was estimated by the surface tension

TABLE II
Estimated Surface Tension of Polymers at the Mixing Temperature (255°C)

Polymer	$\gamma_i = A - BT$ (°C)	Polarity[a]	γ_i[b] mN/m	γ_i^p mN/m	γ_i^d mN/m	Ref.
PP	30.5–0.056T	0.021	29.65	6.55	23.097	3,30,31
PC	44.1–0.06T	0.246	21.7	0.54	21.15	32
SEBS	34.56–0.045T	0.002	22.95	1.60	21.34	3,30,31

[a] Polarity is independent of temperature.
[b] $\gamma_i = \gamma_i^p + \gamma_i^d$.[29]

data of EB. Table III summarizes the interfacial tension between polymer pairs. The spreading coefficients $\lambda_{C/B}$, $\lambda_{B/C}$ and RIE model are calculated using equations 1–5 and presented in Tables IV and V.

According to data calculated for sample I1 (Tables IV and V), the spreading coefficients $\lambda_{B/C}$ and $\lambda_{C/B}$ are both negative and also the morphology in which the C-phase encapsulates the B-phase has the lowest value of RIE. According to the concept of the spreading coefficient B and C phases remain separate and according to the RIE model, SEBS is expected to encapsulate PC. Thus, calculations demonstrate a small driving force for the PC to encapsulate the SEBS. However, Figure 1 shows a disagreement between the prediction of phase morphology from the model predictions and the phase morphology observed via SEM in this sample. This effect could be attributed to the formation complex microstructure (core-shell and individual particles). In fact, this complex morphology can not be explained by mentioned models exactly. Considering all of the above, other microstructures that observed in other samples and also the effect of SEBS-*g*-MAH presence were not considered by these models.

Morphological study

SEM micrographs of the samples with different weight ratios of SEBS to SEBS-*g*-MAH according to Table I, are shown in Figure 1. As it can be seen in this figure, PC is encapsulated by the SEBS phase. This is in disagreement with the theoretical prediction based on spreading coefficient but in an agreement with RIE data given in Tables IV and V. Also the results of Image Analysis of these samples are illustrated in Table VI. The blend containing only nonreactive SEBS [Fig. 1(a)], shows PC particles encapsulated by the SEBS phase to form core-shell composite particles, together with two dispersed phases morphology consisting of individual PC and SEBS particles. As it can be seen in Table VI, in Figure 1(a) the number average diameter of core-shell particles is 1.33μm and core size is 0.88 μm. With decreasing the SEBS/SEBS-*g*-MAH weight ratio from 100/0 to 75/25 [Fig. 1(b)], the number average diameter of core-shell particles and PC cores increased from 1.33 to 2.22 μm and 1.21 to 1.40 μm respectively. One can also see that, SEBS individual dispersed domains have been remarkably decreased and less core-shell composite droplets are present within the PP matrix and individual domains of PC have been increased. This trend could be ascribed to the higher affinity of SEBS to the SEBS-*g*-MA in comparison with PC during the addition of SEBS and PC to the PP/SEBS-*g*-MA binary masterbatch in the second stage of melt mixing. Thus, the possibility of core-shell droplet formation decreases leading to an increase in the average size and number of the malformed and irregular individual particles within the PP matrix. This phenomenon is clearly obvious in Figure 1(b) as the enlargement of the dark holes representative of the droplet size, compared with Figure 1(a).At the SEBS/SEBS-*g*-MAH weight ratio of 50/50 [Fig. 1(c)], the size of core-shell particles and PC cores decreased. In this composition, the number of individual PC and core-shell particles increased. At the SEBS /SEBS-*g*-MA weight ratio of 25/75 [Fig. 1(d)] the type of morphology turns to core-shell in which SEBS-*g*-MA encapsulates the PC particles. Thus, this blend formed much smaller core-shell and individual PC particles. Finally, the 0/100 blend (containing only reactive SEBS-*g*-MAH) displayed large core-shell particles. Owing to agglomeration of core-shell particles, SEM micrograph of this sample [Fig. 1(e)] shows improper dispersion of the dispersed phases. According to these results, it could be suggested that SEBS acts more effectively in decreasing the interfacial tension and improving the morphology of PP/PC/SEBS compared withSEBS-*g*-MA. This problem could be a result of lower

TABLE III
Estimated Interfacial Tension at 255°C

Interface	Interfacial Tension at 255°C (mN/m)
PP/SEBS	1.21
PP/PC	7.03
PC/SEBS	6

TABLE IV
Morphology Predicted by Spreading Coefficient Model

Ternary polymer blend	$\lambda_{C/B}$[a]	$\lambda_{B/C}$[a]
PP/SEBS/PC	−0.18	−11.82

[a] C phase is SEBS and B phase is PC.

TABLE V
Relative Interfacial Energies for (70PP/15PC/15SEBS) Ternary Blends

Ternary polymer blend	$x = V_B/V_C$[a]	RIE_{B+C}[a]	$RIE_{B/C}$[a]	$RIE_{B/B}$[a]
70PP/15SEBS/15PC	0.76	7.07	16.2	6.75

[a] C phase is SEBS and B phase is PC.

interactivity(miscibility) between iPP and SEBS-*g*-MAH. Two factors affect the miscibility :MA grafted on EB blocks and molecular weight of copolymer and copolymer blocks. SEBS with higher molecular weight has longer EB blocks, therefore, one could expect better miscibility with iPP, i.e., thicker iPP-EB interfaces and consequently lower interfacial tension between iPP-SEBS than iPP-SEBS-*g*-MAH. Miscibility factors (parameter B as a measure) for iPP/SEBS and iPP/SEBS-*g*-MAH are 1.1 and 0.86 respectively.[15]

Thermal properties

The phase morphology of ternary polymer blends, are quite complex, which inevitably imply there are various reasons affecting crystallization. In PP/PC/SEBS ternary polymer blends, the crystallization of PP is affected by the presence of PC and SEBS, respectively. The solidification of PC particles dispersing in the PP melts results in heterogeneous nucleation, which significantly increases the crystallization temperature of PP. The crystallization temperature was shifted to higher temperatures by addition of SEBS. This demonstrated that SEBS acts as a nucleation agent for PP (heterogeneous nucleation). The encapsulation of PC by SEBS will improve the interfacial adhesion of PP/PC/SEBS ternary polymer blend but reduces the heterogeneous nucleation of PP matrix. Therefore, the crystallization temperature of matrix shifts to lower temperature with the formation of core-shell particles. The compatibilized system also presents the lower melting enthalpy, which indicates the decreasing crystallinity degree of PP blends.[33]

Thermal data of the samples are summarized in Table VII. According to SEM observation, sample I1 containing the finest samples core-shell particles exhibit the lowest crystallinity degree as compared with other samples. This behavior can be attributed to the homogeneous nucleation of core-shell particles [3], because the fine core-shell particles do not contain heterogeneous nuclei and therefore require greater degrees of super cooling. Thus, the Tc of PP matrix shifted to a lesser degree with respect to other blends. This sample shows the lowest melting enthalpy and crystallinity degree, because the interaction between core-shell particles and PP matrix might prohibit the mobility of PP chains that results in reduction of melting enthalpy and crystallinity degree. In sample I2, the number of fine core-shell particles decreased and the number of PC individual particles increased. Therefore in this sample crystallinity degree, melting enthalpy and Tc of the PP increased. In sample I3, the number of PC particles increased but the number of core-shell particles increased and the size of these particles reduced. This effect results in increasing the degree of crystallinity and melting enthalpy and decreasing the Tc of the PP matrix. In samples I4 and I5, the crystallization temperature decreased as the number of PC particles decreased and the number of core-shell particles increased and also melting enthalpy and crystallinity degree decreased as compared with sample I3.

Mechanical properties

Table VIII summarizes the mechanical properties of the ternary blend samples prepared in this study. As a reference, the mechanical properties of PP matrix was measured. All ternary samples exhibited a remarkable rise in the impact strength compared with pure PP, as a sixfold increase was observed in sample I_1 which is attributed to the reinforcing effect of PC and also the toughening effect of SEBS phase. This is confirmed by comparing the relative data with PP/PC and PP/SEBS binary blends. It could be claimed that the SEBS phase is responsible for the high impact strength obtained for the ternary blends. The least impact strength was observed in sample I_3, which was expectable as the consequence of morphology type discussed before. In this sample, the presence of large rod-like composite droplets negatively affects the impact strength. On the other hand, the presence of core-shell particles is likely to increase impact strength, whereas rod-like composite droplets reduce this property. In samples I4 and I5, the larger the disperse phase particles are, the higher the possibility of stress concentration would be, so the impact strength of these sample is expected to be below compared with sample I1 but rod-like composite droplets were not detected. This problem leads to higher impact strength of these samples rather than samples I3. All of the above evidence suggests that this trend can be attributed to differences between the SEBS and SEBS-*g*-MAH effect on impact strength. SEBS has higher molecular weight than SEBS-*g*-MAH and better miscibility with iPP chains that are influential factors on impact resistance (miscibility factors (parameter B as a measure) for iPP/SEBS and iPP/SEBS-*g*-MAH are 1.1 and 0.86, respectively). As it can be seen in Table VI, sample I1 has core-shell composite particles together with two dispersed phase morphology consisting of individual PC and SEBS particles. When SEBS-*g*-MAH was added to PP/PC/SEBS ternary blends, the morphology gradually changed. In sample I2, SEBS-*g*-MAH relocated to the shell of core-shell

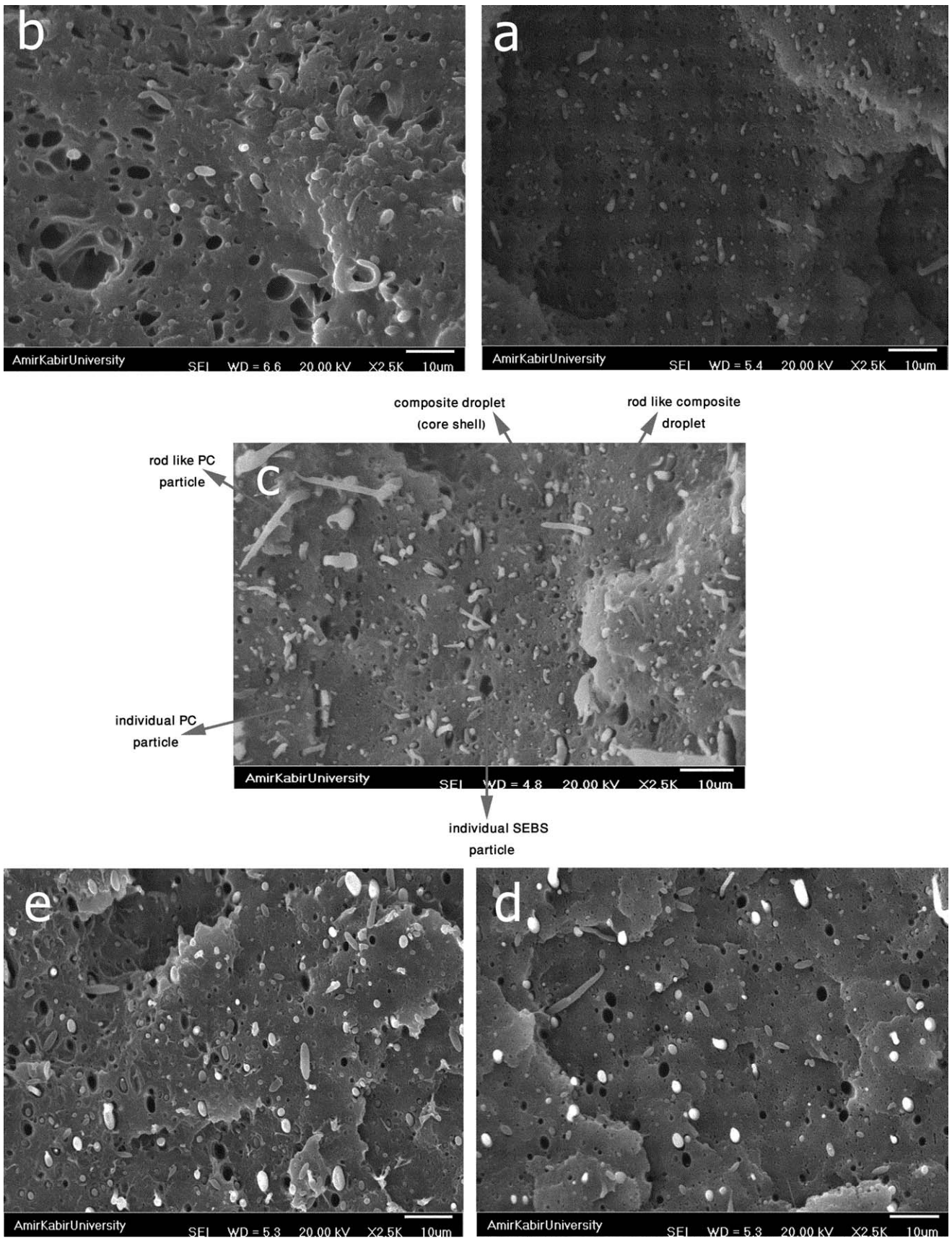

Figure 1 SEM micrographs of PP/(SEBS+SEBS-*g*-MA)/PC samples with SEBS/ SEBS-*g*-MA weight ratio of (a)100/0, (b) 75/25, (c) 50/50, (d) 25/75, and (e) 0/100.

TABLE VI
Results of Image Analysis of SEM Micrographs (I1-I5)

sample code	Number average diameter of individual SEBS particles (μm)	Number of individual SEBS particles	Number average diameter of individual PC particles (μm)	Number of individual PC particles	Number average diameter of composite droplets (μm)	Number of composite droplets	Number average diameter of rod like PC particles (μm)	Number of rod like PC particles	Number average diameter of rod like composite droplets (μm)	Number of rod like composite droplets
I1	0.9325	70	1.2126	5	1.3380789	38	–	–	–	–
I2	2.2878788	33	1.4070417	24	2.2215	10	–	–	–	–
I3	0.9788571	49	0.6556389	36	1.4429	30	1.2571429	7	1.5611724	28
I4	1.3289574	37	0.9174444	27	1.6998542	48	–	–	–	–
I5	1.3227447	47	–	–	1.8245556	45	–	–	–	–

TABLE VII
DSC Results of the PP/PC/SEBS Ternary Blend Samples

	DSC			
Sample code	Tc (°C)	ΔHf (J/gr)	wpp	Xc (%)
Pure PP	108.2 ± 1.402	76.67	1	36.65
I1	109.2 ± 1.407	63.15	0.7	43.12
I2	111.2 ± 1.39	71.04	0.7	48.50
I3	110.5 ± 1.38	72.61	0.7	49.58
I4	110.1 ± 1.28	64.58	0.7	44.09
I5	110.8 ± 1.54	64.9	0.7	44.31

particles and the shell becomes thicker and this blend exhibited large core-shell particles with large individual particles. In sample I3, rod-like composite droplets were appeared that SEBS-*g*-MAH may contribute to shell formation of these particles. Sample I4, exhibited large core-shell particles but rod-like composite droplets that can negative effect on the impact strength disappeared. Finally, sample I5 showed a smoother morphology consisting of large core shell particles. In this sample, SEBS-*g*-MAH contributes to thickening of shell in core-shell particles. It is also observed that a number of core-shell particles form agglomerates.

Investigation of the modulus data (Table VIII) shows that, the modulus of ternary blend samples is mostly affected by the type of the morphology of these samples. As discussed above, in sample I1, SEM showed the disperse phase morphology to be dominantly individual small core-shell particles to resulting a drop in experimental modulus values. Similarly, the reinforcing effect of individual PC particles and rod-like composite droplets are shown by the greater modulus retention of sample I3. The yield stress is controlled by several factors such as, volume fraction, average diameter, and size distribution of dispersed phases and interfacial adhesion between disperse and matrix phases.[34] The combined effect of PC and SEBS dispersed phases in PP/PC/SEBS ternary blend can change greatly the

TABLE VIII
Mechanical Properties of the PP/PC/SEBS Ternary Systems

Sample code	Impact strength (J/m)	Yield stress (MPa)	Modulus (MPa)
Pure PP	25.66 ± 0.471	32.3 ± 0.39	1167 ± 22.6
PP/PC (70/30% wt)	34 ± 5.66	37.23 ± 1.01	1709.32 ± 63.63
PP/SEBS (70/30% wt)	551.33 ± 13.58	23.33 ± 0.32	896.06 ± 4.14
I_1	151 ± 2	25.64 ± 0.00	967.61 ± 74.24
I_2	129 ± 15	26.29 ± 0.57	1016.77 ± 96.51
I_3	117 ± 20	27.01 ± 0.64	1188.34 ± 54.69
I_4	136 ± 1	26.03 ± 0.37	984.15 ± 5.25
I_5	131 ± 8	25.79 ± 0.28	1018.17 ± 80.56

yield stress of PP matrix. In sample I1, because of the fine dispersion of composite droplets and smaller size of these particles compared with other samples, the yield stress showed a minimum in the region of 100/0 SEBS to SEBS-*g*-MAH. In contrast, the sample I3 exhibited large core-shell particles, rod-like composite droplets and also individual PC droplets cause increased the yield stress. But, the PC dispersed phases have not significant reinforcing effect at higher strain so the difference between the yield stress value of this sample and other samples (especially sample I1) is not very high.

CONCLUSIONS

The ternary polymer blends based on PP/PC/SEBS explained in this research work produced very different phase morphologies compared with other ternary systems. These variations in phase morphology can be attributed to adding SEBS-*g*-MAH, and finally showed a wide range of mechanical properties. SEM showed the blend containing only nonreactive SEBS, PC particles encapsulated by the SEBS phase to form core-shell composite particles, together with two dispersed phase morphology consisting of individual PC and SEBS particles. When SEBS-*g*-MAH is incorporated into the blend, the type of morphology and the size of dispersed phases changed from core-shell composite particles to a mixed of core-shell composite particles, individual particles and rod-like composite particles. DSC results showed that the blends containing only SEBS, the lowest PP crystallinity percentage and minimum value of crystallization temperature were observed. This effect can be attributed to the homogeneous nucleation of core-shell particles. Mechanical properties showed that the variation in these properties with increasing SEBS-*g*-MAH %wt was shown to reflect the changes in dispersed phase morphology (i.e., type of morphology, volume fraction, average diameter and size distribution of dispersed phase, and interfacial adhesion).Also, these variations can be attributed to reinforcing effect of PC and toughening effect of SEBS components. Finally, the change in dispersed phase morphology promoted by adding the SEBS-*g*-MAH has generated a range of PP ternary blends with higher impact strength and modulus compared with PP matrix(sample I3), but lower yield stress to the PP base.

References

1. Fung, K. L; Lie Robert, K. Y. Polym Test 2006, 25, 923.
2. Sung, Y. T; Han, M. S; Hyun, J. C; Kim, W. N. Polymer 2003, 44, 1681.
3. Wilkinson, A. N.; Clemens, M. L.; Harding, V. M. Polymer 2004, 45, 5239.
4. Ohlsson, B.; Hassander, H.; Tornell, B. Polymer 1998, 39, 26, 6705.
5. Wilkinson, A. N.; Laugel, L; Clemens, M. L.; Harding, V. M. Polymer 1999, 40, 4971.
6. Tucker, J. D.; Lee, S.; Einsporn, R. L.,Polym Eng Sci 2000, 12, 2577.
7. Kalfoglou, N. K; Samios, C. K; Papadopoulou, C. P.,J Appl Polym Sci 1998, 68, 589.
8. Yin, Z; Zhang, Y.; Zhang, X.; Yin, J. Polymer 1998, 39, 547.
9. Huang, J. J.; Keskkula, H.; Paul, D. R. Polymer 2006, 47, 624.
10. Wang, P.; Meng, K.; Cheng, H.; Hong, S.; Hao, J.; Han, C. C.; Haeger, H. Polymer 2009, 50, 2154.
11. Yin, L.; Yin, J.; Shi, D.; Luan, S. Eur Polym J 2009, 45, 1554.
12. Wang, B. B.; Wei, L. X.; Hu, G. S. J Appl Polym Sci 2008, 110, 1344.
13. Kusmono Ishak, Z. A. M.; Chow, W. S.; Takeichi, T.; Rochmadi. Composites (Part A), 2008, 39, 1802.
14. Denac, M.; Smit, I.; Musil, V. Composites (PartA), 2005, 36, 1094.
15. Denac, M.; Smit, I.; Musil, V. Composites (PartA), 2005, 36, 1282.
16. Guo, H. F.; Packirisamy, S.; Gvozdic, N. V.; Meier, D. J. Polymer 1997, 38, 4, 785.
17. Luzinov, V. I.; Xi, K.; Pagnoulle, C.; Huynh-Ba, G.; Jerome, R. Polymer 1999, 40, 2511.
18. Luzinov, V. I.; Pagnoulle, C.; Jerome, R. Polymer,2000, 41, 3381.
19. Luzinov, V. I.; Pagnoulle, C.; Jerome, R. Polymer 2000, 41, 7099.
20. Kim, B. K; kim, M. S. J Appl Polym Sci 1993, 48, 1271.
21. Ha, M. H; Kim, B. K. J Appl Polym Sci,2004, 91, 4027.
22. Nemirovski, N.; Siegmann, A.; Narkis, M. J Macrom Sci Phys 1995, 34, 459.
23. Hobbs, S. Y.; Dekkers, M. E. J.; Watkins, V. H. Polymer 1988, 29, 1598.
24. Reignier, J.; Favis, B. D. Macromolecules 2000, 33, 6998.
25. Hemmati, M.; Nazokdast, H.; Panahi, H. S.;J Appl Polym Sci 2001, 82, 1129.
26. Valera, T. S.; Morita, A. T.; Demarquette, N. R. Macromolecules 2006, 39, 2663.
27. Reignier, J.; Favis, B. D.; Heuzey, M. C. Polymer 2003, 44, 49.
28. Chow, W. S.; Mohd Ishak, Z. A.; Karger-Kocsis, J.; Apostolov, A. A; Ishiaku, U. S. Polymer 2003, 44, 7427.
29. Wu, S. Polymer interface and adhesion; Marcel Dekker: New York, 1982; Chapter 3.
30. Potschke, P; Pionteck, J; Stutz, H. Polymer 2002, 43, 6965.
31. Menke, T; Funke, Z; Maier, R; Kressler, J. Macromolecules 2000, 33, 6120.
32. Brandrup, J.; Immergut, E. H; Grulke, E. A. Polymer Handbook, 4th ed.; Wiley: New York, 1999.
33. Dai, S.; Ye, L. J Appl Polym Sci 2008, 108, 3531.
34. Bai, S. L; Wang, G. T; Hiver, J. M., G'Sell, C. Polymer 2004, 45, 3063.